Molecular Biology Reports (2024) 51:467
https://doi.org/10.1007/s11033-024-09315-w

ORIGINAL ARTICLE

Osteosarcoma cells exhibit functional interactions with stromal cells, fostering a lung microenvironment conducive to the establishment of metastatic tumor cells

Matías J. P. Valenzuela Alvarez[1] · Luciana M. Gutierrez[1] · Juan M. Bayo[2] · María J. Cantero[2] · Mariana G. Garcia[2] · Marcela F. Bolontrade[1]

Received: 7 November 2023 / Accepted: 2 February 2024

Abstract

Background Osteosarcoma (OS) stands out as the most common bone tumor, with approximately 20% of the patients receiving a diagnosis of metastatic OS at their initial assessment. A significant challenge lies in the frequent existence of undetected metastases during the initial diagnosis. Mesenchymal stem cells (MSCs) possess unique abilities that facilitate tumor growth, and their interaction with OS cells is crucial for metastatic spread.

Methods and results We demonstrated that, in vitro, MSCs exhibited a heightened migration response toward the secretome of non-metastatic OS cells. When challenged to a secretome derived from lungs preloaded with OS cells, MSCs exhibited greater migration toward lungs colonized with metastatic OS cells. Moreover, in vivo, MSCs displayed preferential migratory and homing behavior toward lungs colonized by metastatic OS cells. Metastatic OS cells, in turn, demonstrated an increased migratory response to the MSCs' secretome. This behavior was associated with heightened cathepsin D (CTSD) expression and the release of active metalloproteinase 2 (MMP2) by metastatic OS cells.

Conclusions Our assessment focused on two complementary tumor capabilities crucial to metastatic spread, emphasizing the significance of inherent cell features. The findings underscore the pivotal role of signaling integration within the niche, with a complex interplay of migratory responses among established OS cells in the lungs, prometastatic OS cells in the primary tumor, and circulating MSCs. Pulmonary metastases continue to be a significant factor contributing to OS mortality. Understanding these mechanisms and identifying differentially expressed genes is essential for pinpointing markers and targets to manage metastatic spread and improve outcomes for patients with OS.

Keywords Osteosarcoma · Metastasis · Migration · Invasion · Mesenchymal stem cells · Mesenchymal stromal cells

Abbreviations

BM	Bone marrow
CCL2	C–C motif chemokine ligand 2
CCR2	C–C motif chemokine receptor 2
CM	Conditioned medium
CTSA	Cathepsin A
CTSD	Cathepsin D
CTSs	Cathepsins
CXCR4	C–X–C motif chemokine receptor 4
CXCL12	C–X–C motif chemokine ligand 12
DAPI	4′,6-Diamidino-2-phenylindole dihydrochloride

✉ Marcela F. Bolontrade
marcela.bolontrade@hospitalitaliano.org.ar

Matías J. P. Valenzuela Alvarez
valenzuelamatias25@gmail.com

Luciana M. Gutierrez
lucianagutierrez1987@gmail.com

Juan M. Bayo
jmbayo@hotmail.com

María J. Cantero
canter.ma@yahoo.com.ar

Mariana G. Garcia
mggarcia24@gmail.com

[1] Remodeling Processes and cellular niches laboratory, Instituto de Medicina Traslacional e Ingeniería Biomédica (IMTIB)–CONICET-Hospital Italiano Buenos Aires (HIBA)-Instituto Universitario del Hospital Italiano (IUHI), 4240, C1199ACL Potosí, CABA, Argentina

[2] IIMT–CONICET, Facultad de Ciencias Biomédicas, Universidad Austral, Av. Perón 1500, EPB1629AHJ Pilar, Argentina

Published online: 29 March 2024

DiR	1,1′-Dioctadecyl-3,3,3′,3′-tetramethylindotricarbocyanine iodide
DMEM	Dulbecco's modified eagle's medium
DMEM/F12	Dulbecco's modified eagle's medium/nutrient mixture F12
ECM	Extracellular matrix
FBS	Fetal bovine serum
FI	Fluorescence intensity
GAPDH	Glyceraldehyde-3-phosphate dehydrogenase
GEO	Gene expression omnibus
HMEC-1	Human microvascular endothelial cells
IACUC	Institutional Animal Care and Use Committee
IL-1	Interleukin 1 alpha
i.v.	Intravenously
MMPs	Metalloproteinases
MMP2	Metalloproteinase 2
MMP9	Metalloproteinase 9
MSCs	Mesenchymal stem/stromal cells
NIH	National Institutes of Health
qPCR	Real time polymerase chain reaction
PBS	Phosphate buffer solution
PECAM	Platelet–endothelial cell adhesion molecule 1
OS	Osteosarcoma
SDS-PAGE	Sodium dodecyl sulfate polyacrylamide gel electrophoresis

Introduction

A pivotal aspect of malignant tumor progression is the emergence of detectable metastasis, a significant clinical challenge in cancer treatment. Migration and invasion are two key biological processes that underpin and facilitate the dissemination of tumor cells from the primary site. While intricately interconnected and occasionally converging towards the same biological objective, these processes possess distinct features. Hanahan and Weinberg have identified tissue invasion and metastasis as hallmarks features of cancer, and Labeznik highlighted their critical role in distinguishing benign from malignant tumors in 2010 [1–3]. Invasion involves a complex biological interplay, predominantly orchestrated by proteins capable of modifying the extracellular matrix (ECM), such as metalloproteinases (MMPs) or cathepsins (CTSs) [4, 5]. For tumor cells to spread to distant sites, cell migration is imperative, regulated by various chemotactic axes like CXCR4–CXCL12 or CCR2–CCL2 [6–8]. Metastasis, representing the advanced stage of cancer spread, stands as the primary cause of mortality and morbidity, contributing to 90% of cancer-related deaths [9]. Consequently, tumors characterized by rapid progression and metastatic capabilities assume considerable significance in this context.

Osteosarcoma (OS) stands out as the most prevalent bone tumor, with a predominant pulmonary metastasis pattern. The presence of OS metastases occurs early in the progression of the tumor. Even in cases where twenty percent of OS patients receive an initial diagnosis of metastatic OS, it is estimated that a substantial 80% of OS patients harbor undiagnosed micrometastasis at the time of diagnosis [10–14]. Despite advances since the 1970s, the 5-year survival rate for patients with metastatic OS disease has not presented significant improvement, remaining in the range of 15–30%. The emergence of micrometastases poses a substantial challenge, given their elusiveness to conventional methods [15].

Given the tissue context of OS, particular attention is drawn to mesenchymal stem/stromal cells (MSCs), which play a significant role in various aspects. MSCs, being multipotent stem cells, possess characteristics that make them conducive to supporting tumor growth [16, 17]. Additionally, our prior research has demonstrated that the stromal component within the OS microenvironment influences the stemness state of both tumor cells and MSCs, with adjustments according to the specific tumor context [18, 19]. Due to their versatile nature, MSCs have been implicated in numerous cancer models, participating in nearly all cancer hallmarks and underscoring their role as integral components of the tumor microenvironment [1, 20, 21]. The pathological bone scenario established during the onset and progression of OS involves intricate signaling and molecular exchanges between tumor cells and the altered bone niche. As OS progresses to pulmonary metastasis, tumor cells within the primary site may acquire traits associated to metastasis, such as enhanced migratory and invasive capacities. Simultaneously, the dynamic alterations in the stroma might exert a selection pressure on pre-existing OS subpopulations, favoring cells with metastatic traits to leave the nest towards potential metastatic locations.

In this schema, our primary focus has been on the interconnected modulation between MSCs and OS cells, examining the resulting migratory patterns in both primary and metastatic settings. In vitro, we demonstrated that MSCs exhibit a migratory pattern favoring a response to the secretome of non-metastatic OS cells. When challenged to secretomes from lungs pre-loaded with OS cells, MSCs exhibited a migratory response directed towards lungs colonized with metastatic OS cells. Previous studies from our group have established that MSCs integrate into various tumor stromas [22, 23]. To contextualize this migratory response towards a complex secretome, our model illustrated that MSCs not only migrate but also home in OS lung metastatic areas. This proof of concept emphasizes the crucial role of MSCs as supportive stromal components in the metastatic progression of OS, suggesting that categorizing a cell or group of cells

as metastatic or non-metastatic by eliciting a given biological response within their immediate surrounding conditions, is ultimately modulated by the whole niche. Additionally, metastatic OS cells exhibited an elevated migratory response towards MSCs' secretome. This feature was accompanied by an increased production of pro-metalloproteinase 2 (pro-MMP2) and cathepsin D (CTSD), as well as the release of active MMP2 by metastatic OS cells. Cancer progression involves multistep functional events, culminating in the acquisition of a metastatic phenotype. Our assessment focused on two complementary tumor capacities relevant to metastatic spread, highlighting the importance of inherent cell features enabling colonization of a distant organ. Simultaneously, it underscored the significance of niche-wide signaling integration. This suggests that the interplay of migratory responses between OS cells already established in the lungs, prometastatic OS cells in the primary tumor, and circulating MSCs is pivotal for the successful growth of secondary tumors. Hence, the metastatic secretome proved capable of inducing a differential migratory response in MSCs. Moreover, the MSCs' secretome induced differential migration in OS cells with distinct metastatic abilities. Pulmonary disease remains as decisive factor in OS mortality, and identifying mechanisms and differentially expressed genes associated with metastasis holds promise for discovering markers and targets for therapeutic interventions in OS metastatic spread.

Materials and methods

Cell lines

Human OS cell lines were generously provided by Dr. Kleinerman from MD Anderson Cancer Center (MDACC). The cells were cultured in Dulbecco's Modified Eagle Medium: Nutrient Mixture F12 (DMEM/F12), supplemented with 2 mM L-glutamine, 100 U/mL penicillin, 100 mg/mL streptomycin (Invitrogen), and 10% fetal bovine serum (FBS; Natocor). Cultures were maintained at 37 °C with 5% CO_2. Two distinct OS cell lines were employed: SAOS2, established from a primary tumor in the seventies, and LM7, a subline derived from parental SAOS2 cells, selected for its metastatic ability through lung cyclic circulation. This ability is associated to with the evasion of apoptosis and apoptosis-resistance mechanisms [24]. Human microvascular endothelial cells HMEC-1 (provided by Dr. Candal, Centers for Disease Control, Atlanta) were cultured in DMEM/F12 supplemented with 10% FBS (Natocor), 2 mM L-glutamine, 100 U/mL penicillin, and 100 mg/mL streptomycin. Human MSCs were isolated from bone marrow (BM) aspirates collected from posterior iliac crest of healthy donors for BM transplantation after obtaining informed consent (Institutional Review Committee approval #1497). Mononuclear cells, collected from Ficoll–Hypaque gradient (Sigma-Aldrich) were plated in low-glucose DMEM (DMEM low, Invitrogen), with 20% FBS (Internegocios S.A.). MSCs utilized in the experiments were from passages 2 to 4 [22]. Mycoplasma species verification was conducted using the MycoAlert Mycoplasma Detection Kit (Lonza Inc.).

Cell conditioned medium

The cellular secretome compartment is represented by its conditioned medium (CM). Cells were seeded in 100 mm culture dishes and grown to 80% confluence, followed by washing with phosphate-buffered solution (PBS). Subsequently, cells were cultured for 24 h with basal medium (DMEM or DMEM/F12 depending on the cell type) without FBS to avoid contamination with serum proteins. After this period, the CM was collected by aspiration to minimize cell disruption and contamination with intracellular proteins, followed by centrifugation for 5 min at 1200 rpm. Collected CM was aliquoted and stored at − 80 °C until its use in functional assays. To obtain CM derived from mice lungs, 4 to 6-week-old athymic nude mice (nu/nu, NIH) were injected intravenously (i.v., lateral tail vein) with 1×10^6 LM7 or SAOS2 cells/200 µL PBS resulting in the development of microscopic lung metastases (LM7 cells) or not (SAOS2 cells). The control group received 200 µL of physiological solution i.v. (lateral tail vein). After 5 weeks mice were sacrificed, and lungs were dissected (approval of the Institutional Animal Care and Use Committee, IACUC IMTIB 0001/19). Lungs were minced into pieces smaller than 1 mm^3 and transferred to a 24-well tissue culture plate (6 fragments/well) with 500 µL of complete DMEM without FBS. After 24 h, the CM was harvested, centrifuged at 1200 rpm, aliquoted, and stored at − 80 °C until its use in functional assays.

In vitro migration assays

For in vitro cell migration assays, cells were cultured as specified previously (cell lines). Cell migration was assessed using a modified Boyden chamber (Neuroprobe Inc.). Cells were cultured until reaching 70–90% confluence, and serum starvation was performed for 24 h. After this, cells were seeded on the upper wells of the chamber (1.2×10^4 cells/50 µL DMEM). The chemotactic stimulus was added in the lower wells (28 µL). The cells responding to chemotactic stimuli migrated through an 8-µm-pore polycarbonate filter located between the upper and lower wells (Neuroprobe Inc.). Basal medium served as the negative control. Migration was evaluated over a 4-h period at 37 °C. Post-assay, cells on the upper side of the filter were scraped-off using a razor blade. The cells attached to the lower side

were fixed using 4% paraformaldehyde (PFA) and stained with 4,6-diamidino-2-phenylindole dihydrochloride (DAPI, Sigma-Aldrich) to allow visualization of cell nuclei. Fluorescent images were captured from two visual fields covering the entire well using fluorescent-field microscopy (Olympus). Cell counting was carried out through the presence of cell nuclei, providing the mean number of cells/field ± SD), using ImageJ software (National Institutes of Health, NIH, Bethesda, MD).

Gelatin zymography assay

To assess gelatinolytic activity, 5×10^4 cells were seeded in 24-well plates. When cells reached 80% confluence, they were washed with PBS and cultured in serum-free DMEM with 1 g/L glucose for 6 h before collecting supernatants. The positive control consisted of CM from HT1080 cells. MMP2 and MMP9 activity were determined through zymography. In brief, cell culture supernatants (40 µL) were run on a 10% sodium dodecyl sulfate polyacrylamide gel electrophoresis (SDS-PAGE) system containing 0.1% gelatin (Sigma-Aldrich). The gel was stained with Coomassie Brilliant Blue R-250 for30 min at room temperature. Gelatinase activity was visualized through negative staining, and gel images were captured using a digital camera (Canon EOS 5D). Densitometry analysis was performed using Scion Image software from Scion Corporation, MD. Relative pro and active-MMP2 values were obtained by normalizing the values to positive control samples (CM of HT1080).

Reverse transcription-polymerase chain reaction (RTPCR) and real time polymerase chain reaction (qPCR)

Total RNA was extracted from OS cells using Trizol Reagent (Molecular Research Center, USA). Subsequently, reverse transcription of 2 µg RNA was carried out with 200 U of *Easy Script* Reverse Transcriptase (Transgenbiotech) using Oligo (dT) primers (500 ng). The resulting cDNAs underwent quantitative PCR (qPCR) analysis on aCFX96 Touch TM Real-Time PCR Detection System (Bio-Rad). mRNA levels of Cathepsin A (CTSA), Cathepsin D (CTSD) and Matrix Metalloproteinase-2 (MMP2) were quantified using SYBR Green(Roche) with the following primers: CTSA forward 5′ACGCCAGCCAACTGTGATCCT3′, reverse 5′ATA TGCGGCATCCACGCCTGAA3′; CTSD forward 5′ ACA AGATGTGGGCCTTGCAAGA3′, reverse 5′AAAACGCAG TGCTCCCAGGATA3′; MMP2 forward 5′CCAGCCAGA AGCGGAAACTT3′, reverse 5′ TGACCTTTCCAGCAG ACACC3′. PCR amplification involved an initial cycle at 95 °C for 10 min, followed by 40 cycles with the following parameters: 95 °C for 20 s, 60 °C for 1 min, 72 °C for 40 s and 95 °C for 20 s. A final cycle involved an increase in temperature from 60 to 95 °C (at a rate of 2 °C/min), with fluorescence measured every 15 s to construct the melting curve. Values were normalized to glyceraldehyde-3-phosphate dehydrogenase (GAPDH) mRNA levels, using the following primers: forward 5′ GGGGCTGCCCAGAACATC AT 3′, reverse 5′ GCCTGCTTCACCACCTTCTTG 3′. Data were processed using the DDCt method. Each assay included a non-template control (NTC), and all determinations were performed as triplicates in three separated experiments.

In vivo assays

Animal experiments were conducted with the approval of the Institutional Animal Care and Use Committee (IACUC IMTIB 0001/19). Four to six-week-old athymic male nude mice were i.v. injected with 1×10^6 LM7 cells in 200 µL PBS via the lateral tail vein, resulting in the development of microscopic lung metastases. MSCs were labeled with 1,1′-dioctadecyl-3,3,3′,3′-tetramethylindotricarbocyanine iodide (DiR), an infrared lipophilic tracker (Invitrogen) following the manufacturer's instructions. DiR^+ MSCs ($0.5x10^6$ cells in 200 µL PBS) were administered i.v.10 weeks after the injection of tumor cells. The biodistribution and homing analysis of MSCs were assessed in real-time. DiR in vivo tracking detection was performed using fluorescence imaging (FI) on the IVIS Lumina Bioluminometer (Xenogen). For FI analysis, captured images were quantified as average photons per second per square centimeter per steradian ($p/s/cm^2/sr$).

Bioinformatics analysis

The GSE14359 dataset was retrieved from the Gene Expression Omnibus (GEO) database (https://www.ncbi.nlm.nih.gov/gds/). This dataset comprises mRNA data obtained from 5 frozen conventional osteosarcoma samples, 4 osteosarcoma lung metastases tumor samples, and mRNA from fresh primary osteoblast cells. Each sample was analyzed induplicate. To analyze and visualized specific genes from the GSE14359 dataset, the R2 program (http://r2.amc.nl) was utilized. The specific dataset used for analysis was Mixed Osteosarcoma—Guenther—20—MAS5.0—u133a (also GSE14359 from GEO database) [25]. Gene expression was examined based on primary versus metastatic status and expression data of the samples were shown as individual values categorized by type of sample and the median values of the groups were shown as boxplots graphs in Fig. 2E. Additionally, Kaplan-Meier survival curves for metastasis-free survival rates were generated using the R2 program. This analysis was based on the dataset Mixed Osteosarcoma (Mesenchymal)—Kuijjer—127—vst—ilmnhwg6v2 (also GSE42352 from GEO database) [26].

Statistical analysis

To establish 95% confidence intervals (CI), arithmetic mean values and variance (standard deviation, SD) were calculated based on three independent experiments. Statistical analysis were conducted using unpaired 2-sided Student's t-test for two-groups comparisons and analysis of variance (ANOVA) followed by post-tests Kruskal-Wallis and Dunn's post-tests for comparisons involving more than two experimental groups. The statistical analysis was performed using GraphPad Prism Software, San Diego, CA.A p value < 0.05 was considered statistically significant in all analysis.

Results

Chemotactic crosstalk between parenchymal and stromal cell in OS

To evaluate the impact of SAOS2 and LM7 cells on functions relevant to the cell stromal compartment, the response of MSCs to the CM of OS cell lines was assessed through in vitro migration assays. The results demonstrated that MSCs responded to chemotactic signals present in both SAOS2 and LM7 CM (Fig. 1A). However, SAOS2 cells' secretome induced a 1.5-fold significantly higher chemotactic effect on MSCs compared to the migration exerted by LM7 cells' secretome. This heightened chemoresponse towards the non-metastatic cell line was observed in other stromal cells as well. Human microvascular endothelial cells (HMEC-1) exhibited a similar trend, with a 1.3-fold increased chemotactic response towards SAOS2 secretome (Fig. 1B). Conversely, when OS cells were challenged with the chemotactic stimuli from MSCs, LM7 cells demonstrated a 2-fold increase in their migratory response towards MSC's secretome compared to SAOS2 cells (Fig. 1C).

In vivo context complexity signaling determines migration of stromal populations

To assess the potential impact of the microenvironment, we investigated the chemotactic effect of CM from lungs of animals previously injected with SAOS2 (CML+S) or LM7 (CML+L) cells using in vitro migration assays (Fig. 2A). Interestingly, in contrast to the results obtained from CM under cell-only in vitro conditions, MSCs exhibited a significantly higher chemotactic response towards CM from lungs with LM7 cells compared to CM from lungs with SAOS2 cells (1.69-fold vs 1.06, CML+L and CML+S respectively) (Fig. 2B, C). Given that this difference might be attributed to the added complexity of the *in vivo* lung microenvironment created by the presence of metastatic cells, we analyzed the GSE14359 dataset, a transcriptomic database of human OS primary and metastatic tissue and normal osteoblasts. Focusing on changes associated with an inflammatory context, we selected four candidates: CXCR4 (C–X–C chemokine receptor type 4), S100A14, IL-1α (interleukin 1 alpha), and PECAM1 (platelet-endothelial cell adhesion molecule 1). These genes are implicated in migration, pulmonary inflammation, overall inflammation, and adhesion, respectively. S100A14 and PECAM1 exhibited significantly higher expression in metastatic samples, while CXCR4 and IL-1α displayed a similar trend but with no statistical significance (Fig. 2D, E).

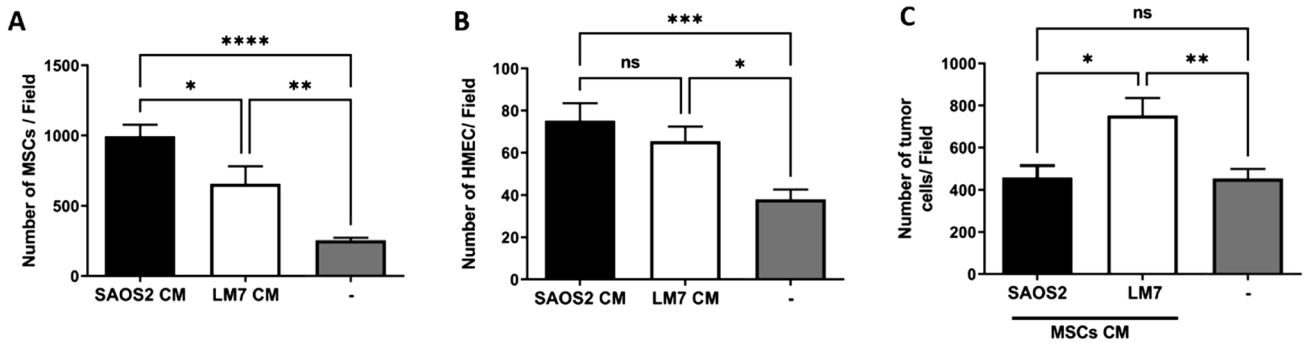

Fig. 1 Chemotactic interplay between parenchymal and stromal cells in OS. **A** The migratory response of MSCs towards the CM of SAOS2 and LM7 cells revealed a significant preference of MSCs for SAOS2 CM, indicating increased migration towards the non-metastatic cell line. **B** The migratory response of HMEC-1 cells towards the CM of SAOS2 and LM7 cells showed no significant differences, suggesting a comparable chemoresponse to both cell lines. **C** The migratory behavior of SAOS2 and LM7 cells towards MSCs' secretome demonstrated that LM7 cells migrated significantly more towards MSCs' CM compared to SAOS2. DMEM was employed as negative control (−) in all migration assays. One-way ANOVA, *ns* no significant; *p < 0.05, **p < 0.01, ***p < 0.001, ****p < 0.0001. The data presented are representative of three independent experiments

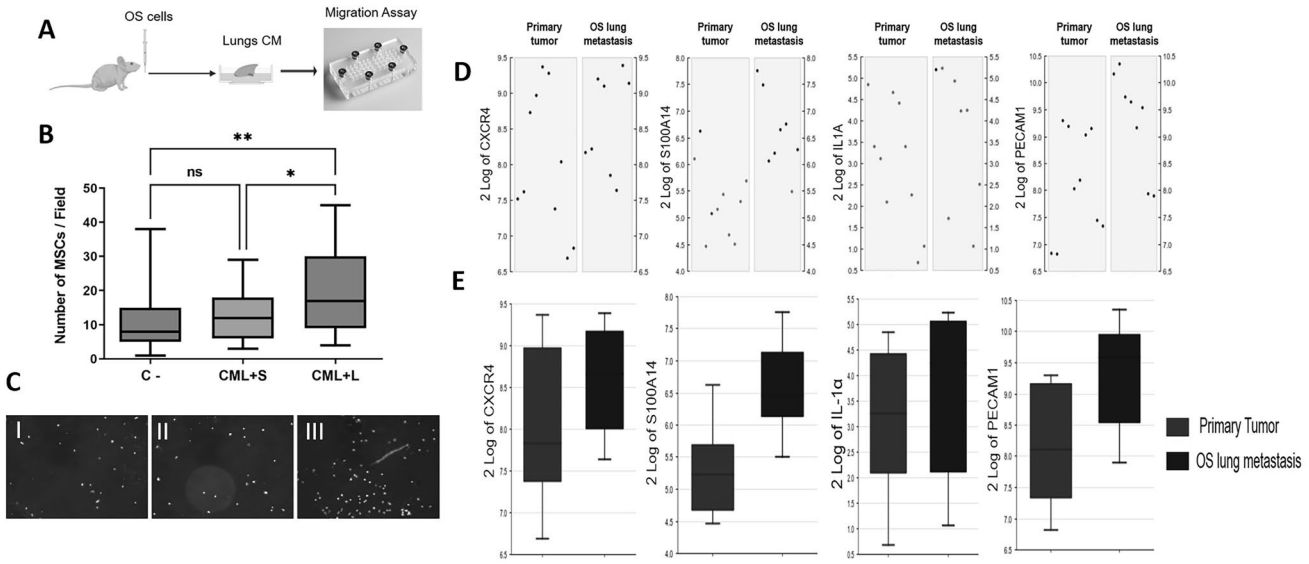

Fig. 2 Migratory response of MSCs to CM from lungs of animals previously injected with SAOS2 or LM7 cells. **A** Schematic illustration of the experimental design of the pulmonary OS metastasis and control groups in nude mice in order to obtain lungs CM. **B** Migration of MSCs towards CM from lungs previously injected with OS cells. CML+S CM from lungs of animals previously injected with SAOS2; CML+L: CM from lungs of animals previously injected with LM7; C-: negative control. **C** Representative images of DAPI stained MSCs migrating in response towards different conditions in B; **I** Negative control (−); **II** CML+S; **III** CML+L. **D** Dot plots of CXCR4, S100A14, IL-1α, and PECAM1 from patients with metastatic OS and non-metastatic patients (GSE14359 dataset). **E** Box plots of CXCR4, S100A14, IL-1α, and PECAM1 from patients with metastatic OS and non-metastatic patients show significantly higher expression in S100A14 and PECAM1 in metastatic samples, while CXCR4 and IL-1α displayed a similar trend (GSE14359 dataset). One-way ANOVA, *ns* no significant; *$p < 0.05$, **$p < 0.01$. Data presented are representative of three independent experiments

Incorporation of systemically delivered MSCs into secondary tumor growth sites

Given the significance of the microenvironment, we investigated the combined impact of the environment and the tumor cell's ability in recruiting MSCs to a metastatic lung site. An in vivo assay was conducted as a proof of concept of the role of the microenvironment as a chemotactic response modulator (Fig. 3A). Within this context, the in vivo migration of MSCs was assessed in lungs with and without metastatic cells. LM7 cells were introduced i.v. into immunosuppressed mice. Pre-labeled MSCs (DiR^+, $0.5–1 \times 10^6$ cells) were i.v. administered 10 weeks after the injection of tumor cells. The biodistribution of MSCs was examined through whole body DiR signal detection (Fig. 3B). The levels of labeled MSCs one-week post-inoculation were notably elevated in the lungs of tumor-bearing mice compared to mice without tumor burden (Fig. 3C, D). This suggests a heightened homing ability of MSCs in the metastatic tumor microenvironment, implying that the presence of LM7 cells within the lungs creates a favorable lung niche, promoting the recruitment of MSCs to the site. Furthermore, the infrared-tagged (DiR^+) MSCs exhibited a heterogeneous distribution within the LM7 lungs, suggesting a chemo-attractive and homing behavior towards localized areas in the lungs bearing tumor cells (Fig. 3C).

Expression and activity of matrix metalloproteinases and cathepsins in OS cells

Tissue remodeling, a crucial aspect in tumor development, encompasses the recruitment of cells both from the local tissue environment and distant tissues. This process plays a pivotal role in establishing a conducive niche for the growth of primary tumors and metastases. A distinctive feature of metastatic cells is their capability to modify and alter the ECM. Aiming to evaluate the capacity of OS cells to modify the ECM, we assessed their ability to secrete active MMPs. Specifically, we analyzed MMP2 and MMP9 activities through zymography of the secretome derived from SAOS2 and LM7 cells. Our findings demonstrated a notable distinction in MMP2 release between non-metastatic and metastatic OS cells. Non-metastatic cells, represented by SAOS2, showed a lack of MMP2 release. In contrast, metastatic LM7 cells exhibited the ability to release both pro and active MMP2 (Fig. 4A–C). Our analysis revealed the absence of MMP9 activity in OS cells. We focused on MMP2 expression in OS cells and found that LM7 cells expressed MMP2 while the parental SAOS2 cells exhibited no significant levels of expression at the mRNA level (Fig. 4D). Interestingly, generation of Kaplan–Meier metastasis-free survival curve using the R2: Genomics Analysis and Visualization Platform (Acad Med Center, Amsterdam) indicated that high MMP2

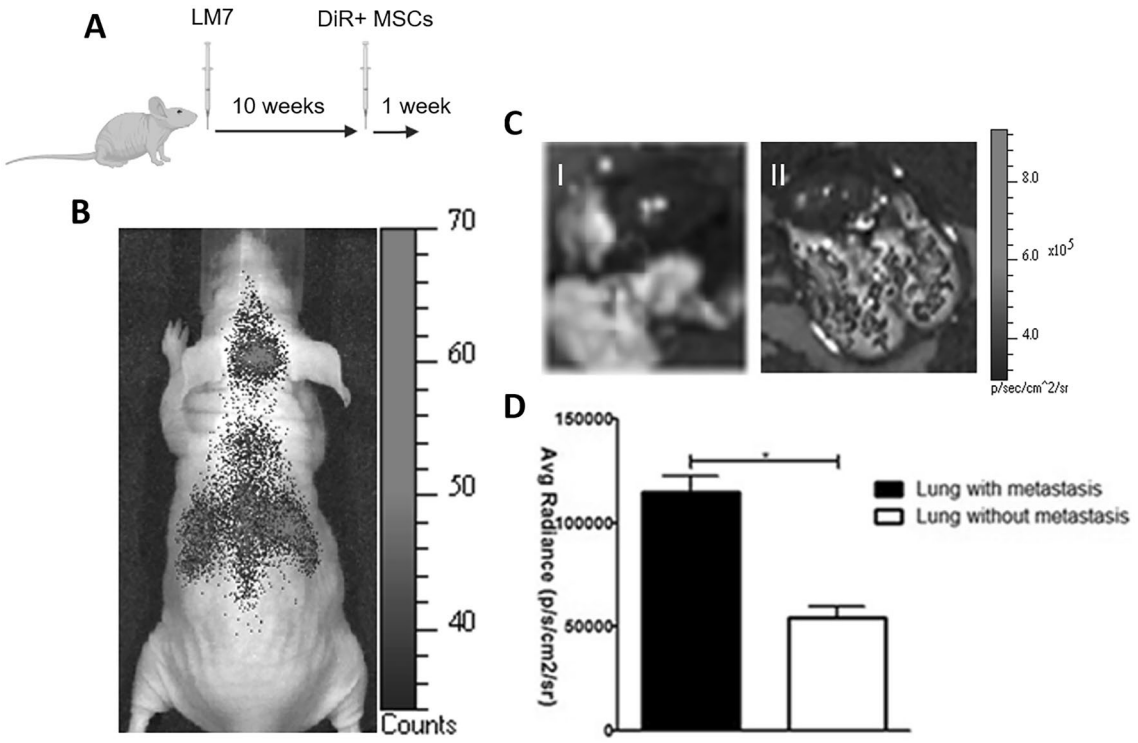

Fig. 3 In vivo biodistribution of MSCs systemically administered 10 weeks after intravenous administration of LM7 tumor cells, analyzed by FI. **A** Schematic illustration of the experimental design depicting the in vivo experimental OS metastasis and MSCs homing ability in the pulmonary environment. **B** Whole-body biodistribution images of DiR pre-labeled MSCs, showcasing the FI signal associated with presence of MSCs in lungs and brain. **C** Representative images of lungs and heart displaying MSCs distribution in control or treated animals; **I** Lungs and heart of a control animal; **II** Lungs and heart of a micrometases-bearing animal. **D** DiR signal detection and quantification (p/s/cm^2/sr) revealed a preferential homing into lungs previously colonized with metastatic cells (*$p < 0.05$). t test, average ± SD

expression was correlated with a diminished metastasis-free survival rate. This suggests a potential role for MMP2 in the establishment of a metastatic niche, emphasizing its significance in OS metastatic spread (Supp. Fig 1). Further, we analyzed the expression of CTSs using qPCR. The results indicated a significant upregulation of CTSD in LM7 cells, with a 3,5-fold increase, while CTSA did not exhibit differences at the mRNA expression levels. These findings suggest that LM7 cells possess a higher expression of molecules functionally associated with ECM remodeling and invasion, further underlining their metastatic characteristics (Fig. 4D).

Discussion

Despite therapeutic advancements, the 5-year survival rate for OS remains at 60–70%, and patients with pulmonary metastases at diagnosis time face a survival rate of 15–30% over the last 30 years [27, 28]. These points at the necessity of understanding the mechanisms of tumor progression in the bone niche as the primary tumor site and the subsequent metastasis that arises from this primary site. Bioinformatics approaches are shaping the personalized era of preclinical and clinical research, but in the case of OS, datasets are often represented by limited cohorts, as compared to other more prevalent cancer types. Despite the limitation of working with smaller datasets, particularly in pediatric tumors like OS, we underscore the potential impact of this approach on future clinical advancements. In this manuscript, we employed a combination of bioinformatics datasets and cellular assays, to illustrate a scenario wherein stromal cells and OS cells interact, leading to the promotion of metastatic traits. In this context, the tumor niche, a complex microenvironment, is established through the intricate interplay among tumor cells, cancer stem cells, stromal cells and the ECM [29]. Notably, MSCs contribute significantly to the stromal compartment, shaping the structural and functional aspects of the microenvironment [17, 21, 30].

Metastasis is a complex biological process encompassing various critical abilities such as invasion, chemotaxis and migration. To understand if the metastatic ability of LM7 cells is functionally linked to other cells within the tumor niche, we investigated the migratory and invasive capacities of both tumor and stromal cells. Metastatic potential often involves the remodeling of the ECM, a key step in the metastatic cascade. Migratory responses play a crucial

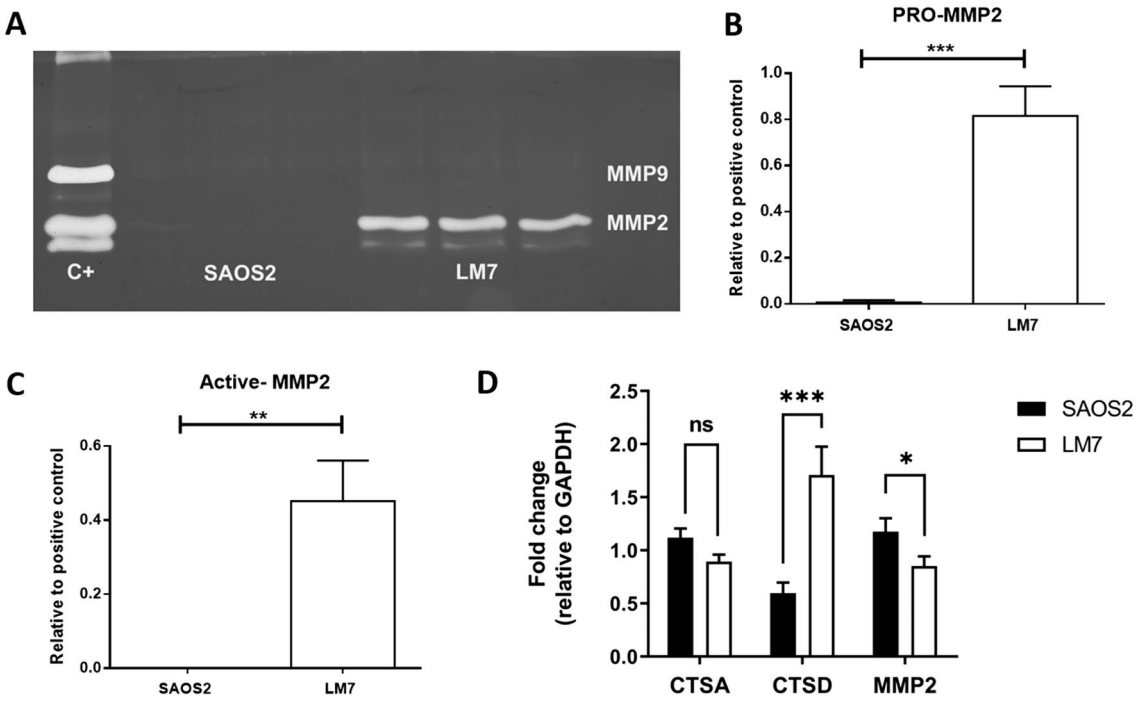

Fig. 4 Characterization of the invasion-related phenotype of OS cells. **A** Metalloproteinase activity in CM from SAOS2 and LM7 cells evaluated by zymography assay. CM from HT1080 cells was used as a positive control (C+). MMP2 was detected, and MMP9 was not detected in the CM from the parental or the metastatic cell line. **B** Pro-MMP2 was significantly higher in the metastatic cell line LM7 than in SAOS2 cells. **C** Active-MMP2 was only present in LM7 CM. **D** qPCR analysis of cathepsin A (CTSA), cathepsin D (CTSD) and MMP2 revealed that LM7 cells had significantly higher CTSD mRNA levels than SAOS2 cells, while CTSA was similar in both cell lines. Regarding MMP2 expression, SAOS2 had higher expression of MMP2 at mRNA level. *T*-test, *ns* no significant, *$p < 0.05$, **$p < 0.01$, ***$p < 0.001$. Data are representative of three independent experiments.

role in tumor progression. Tumor cells heavily rely on an enhanced migratory response for successful metastasis, which involves intra- and extravasation, tissue invasion, and sustaining growth in different anatomic locations [31, 32]. Using a cell-only in vitro approach, we demonstrated that MSCs exhibited a heightened chemoresponse towards the non-metastatic cell line. Interestingly, when challenged with CM from lungs of animals previously injected with OS cells, MSCs exhibited a significantly higher chemotactic response towards lungs with metastatic cells (Fig. 2B, C). On the other hand, LM7 cells exhibited a higher migratory response towards MSCs. This observation is likely linked to the ability of LM7 cells to metastasize, implying that metastatic OS cells home into lungs previously colonized by MSCs. In this scenario, the development of lung metastases could be associated with a permissive niche provided by MSCs previously incorporated into the lungs, lung-residing MSCs, or by exosomes released by tumor-educated MSCs [1, 16, 19]. These results point to the added complexity of the in vivo lung microenvironment, signifying an intricate context for cell migration in vivo. Since the secretome was able to induce a migratory dynamic that could influence the development of metastasis, the question arises if targeting specific components of the secretome could be a promising strategy for therapeutic intervention. Using an expression database of human OS primary and metastatic tissue and normal osteoblasts, we identified molecular candidates involved in signaling cell migration. Specific molecules involved in the interplay between OS cells and the microenvironment, for instance regulatory molecules pertaining to chemotactic axis such as CXCR4, could be a potential therapeutic strategy.

Further, two protein families, MMPs and CTSs, play significant roles in the metastatic cascade. Gelatin zymography was utilized to assess the metastatic potential of LM7 cells by examining the activity of two key enzymes, MMP2 and MMP9. MMP2 and MMP9 have been previously reported to be directly associated with high grade OS and metastatic potential [33]. The demonstrated MMP2-gelatinase activity in the CM from LM7 cells indicates the ability of these cells to produce and secrete active MMP2. In this context, the metastasis-free survival curve of MMP2 indicates that higher expression is associated with a lower probability of metastasis free survival (Supp. Fig. 1). We examined the expression of CTSA and CTSD, two proteins involved in ECM remodeling. Although we observed no differences in

CTSA expression between the cell lines, CTSD was significantly upregulated in LM7 cells. CTSD has been implicated in tumor invasion and metastasis in various tumor models and has also been proposed as a possible biomarker of OS [34–37]. CTSD, which is increased in metastatic cells, has also been reported to play a role in protecting against apoptosis [14]. Our results suggest MMP2 and CTSD as potential therapeutic targets with roles in ECM remodeling and metastasis. The activity associated to MMP2 in metastatic OS cells, can be subject of therapeutic strategies aimed at preventing ECM remodeling. The complexity and the potential redundancy in signaling pathways have to be considered, hence, combination therapies targeting multiple components of the secretome might be more effective [38]. Further studies involving the use of preclinical in vivo models of OS would ensure the validation of these approaches.

In this context, OS cells with advantageous abilities to leave the primary tumor would respond to a permissive "soil" induced by MSCs in the lungs [39–42]. As such, enhanced migration and the ability to degrade ECM were both traits upregulated in metastatic OS cells (Fig. 5). MMP2 has been demonstrated to promote stemness [20, 21]. We had previously shown that metastatic OS cells exhibit an increased capacity to modify the intracellular localization of chemotherapy drugs and a decreased osteoblastic differentiation, traits associated with stemness states [18]. In this scenario, the increased MMP2 in LM7 cells may not only facilitate invasion but also play a role in providing a supportive and favorable environment for the survival of metastatic cells.

While these findings are specific to OS, there are broader implications for understanding common features in tumor microenvironment interactions and metastasis across different cancer types. We emphasize the complexity of the tumor microenvironment, including the interactions among different tumor cell types and stromal cells [29]. These dynamics that are essential in OS, can be regarded as "pan-cancer" characteristics, aligning with the conceptual approach with which cancer hallmarks address tumors [1, 2]. Understanding these processes may provide insights into common mechanisms of metastasis across various cancer types. The differential migratory responses observed in this work may have implications for understanding the interactions between tumor and stromal cells in diverse tumors. The heterogeneity in the primary tumor, regarding metastatic potential, is a common characteristic of many cancers [21, 42]. From our results, a picture emerges depicting a heterogeneous OS primary tumor that avidly recruits stromal cells. Some tumor cell subpopulations would leave the primary tumor and colonize the lungs in response to a suitable niche and stimuli, i.e, lung MSCs, probably further attracting more MSCs to the lungs (Fig. 5). The identification of molecules associated with migration and invasion may have implications for biomarker discovery in other cancers with similar heterogeneity. The identified signaling events mediated by different molecules such as CXCR4, S100A14, IL-1α, and PECAM1, align with the bidirectional migration interplay observed between MSCs and OS cells [17]. Understanding the exposed dynamic interplay between different cell populations in OS, even though specific to this tumor type, may contribute to broader insights into cancer progression and metastasis. Furthermore, the imbalance in bone homeostasis associated with OS onset significantly affects and is affected by MSCs as master regulators of bone physiology [43–46]. A pathologic bone remodeling scenario emerges, with the selection of advantageous properties, resulting in both MSCs and OS cells being able to foster the conditions for a secondary tumor site in a coordinated manner. The identification of novel molecules in OS would permit the validation of molecules with usefulness as a biomarker in a disease in which

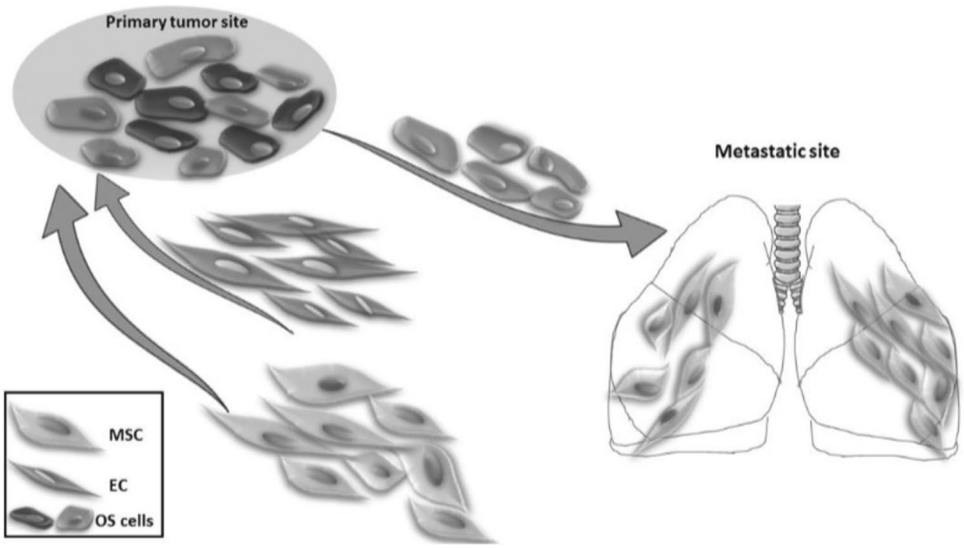

Fig. 5 Proposed model on the interaction of MSCs and endothelial cells with OS cells within the primary site or secondary tumor growth. OS cells residing at the primary tumor site recruit stromal cells, including MSCs and endothelial cells. OS cells with the ability to leave the primary tumor site and colonize new niches exhibit enhanced migration towards MSCs, which have previously colonize the new niche (lung). *MSCs* mesenchymal stem cells, *EC* endothelial cells and *OS cells* osteosarcoma cells

the existence of undetectable lung micrometastases present at diagnosis time remains a critical clinical challenge.

Conclusions

We present a functional and molecular comparison between a parental non-metastatic OS cell line and a derived metastatic cell line selected for lung colonization behavior, proposing a model of OS cells–MSCs interaction at primary and secondary tumor growth sites. Our results demonstrate that subtle molecular modifications in metastatic tumor cells enable lung metastatic colonization. Furthermore, metastatic and non-metastatic OS secretomes differentially modulate the stroma, and OS cells establish a distinct functional interaction with mesenchymal stem cells. Metastatic OS cells create a niche that would ensure tumor establishment in the lungs.

Supplementary Information The online version contains supplementary material available at https://doi.org/10.1007/s11033-024-09315-w.

Author contributions MVA and LMG performed experiments, analyzed data and designed figures. MVA also contributed to the writing of the manuscript and conceived experiments. MJC, MGG, and JB performed experiments; MGG contributed with reagents and analyzed data. MB conceived research and experiments, analyzed data and wrote manuscript. Authors discussed and commented the results on the manuscript.

Funding This work was supported in part by the Fund for Scientific and Technological Research (FONCyT) PICT No. 1974 and by Florencio Fiorini Foundation.

Data availability All relevant data supporting the findings of this study are available within the paper and it's Supporting Information files.

Declarations

Competing interests All authors declare no competing financial interests.

Research involving animals right The animal handling procedures in this study were conducted in accordance with the guidelines and regulations established by the Institutional Animal Care and Use Committee (IACUC) under the protocol number IACUC IMTIB 0001/19. Furthermore, all procedures complied with relevant national and international standards for the ethical use of animals in scientific research. Study design and execution followed the principles outlined in the Guide for the Care and Use of Laboratory Animals published by the National Institutes of Health (NIH).

References

1. Hanahan D (2022) Hallmarks of cancer: new dimensions. Cancer Discov 12(1):31–46. https://doi.org/10.1158/2159-8290.CD-21-1059
2. Lazebnik Y (2010) What are the hallmarks of cancer? Nat Rev Cancer 10(4):232–233. https://doi.org/10.1038/nrc2827
3. Welch DR, Hurst DR (2019) Defining the hallmarks of metastasis. Cancer Res 79(12):3011–3027. https://doi.org/10.1158/0008-5472.CAN-19-0458
4. Vidak E, Javoršek U, Vizovišek M, Turk B (2019) Cysteine cathepsins and their extracellular roles: shaping the microenvironment. Cells 8(3):264. https://doi.org/10.3390/cells8030264
5. Niland S, Riscanevo AX, Eble JA (2022) Matrix metalloproteinases shape the tumor microenvironment in cancer progression. Int J Mol Sci 23:146. https://doi.org/10.3390/ijms23010146
6. Khan SU, Fatima K, Malik F, Kalkavan H, Wani A (2023) Cancer metastasis: molecular mechanisms and clinical perspectives. Pharmacol Ther 250:108522. https://doi.org/10.1016/j.pharmthera.2023.108522
7. Tulotta C, Stefanescu C, Chen Q, Torraca V, Meijer H, Snaar-Jagalska B (2019) CXCR4 signaling regulates metastatic onset by controlling neutrophil motility and response to malignant cells. Sci Rep 9(1):2399. https://doi.org/10.1038/s41598-019-38643-2
8. Xu M, Wang Y, Xia R, Wei Y, Wei X (2021) Role of the CCL2–CCR2 signalling axis in cancer: mechanisms and therapeutic targeting. Cell Prolif 54(10):e13115. https://doi.org/10.1111/cpr.13115
9. Lambert AW, Pattabiraman DR, Weinberg RA (2017) Emerging biological principles of metastasis. Cell 168(4):670–691. https://doi.org/10.1016/j.cell.2016.11.037
10. Marko TA, Diessner BJ, Spector LG (2016) Prevalence of metastasis at diagnosis of osteosarcoma: an international comparison. Pediatr Blood Cancer 63(6):1006–1011. https://doi.org/10.1002/pbc.25963
11. Sheng G, Gao Y, Yang Y, Wu H (2021) Osteosarcoma and metastasis. Front Oncol 11:780264. https://doi.org/10.3389/fonc.2021.780264
12. Strauss SJ, Ng T, Mendoza-Naranjo A, Whelan J, Sorensen PH (2010) Understanding micrometastatic disease and anoikis resistance in Ewing family of tumors and osteosarcoma. Oncologist 15(6):627–635. https://doi.org/10.1634/theoncologist.2010-0093
13. Bruland OS, Høifødt H, Saeter G, Smeland S, Fodstad O (2005) Hematogenous micrometastases in osteosarcoma patients. Clin Cancer Res 11(13):4666–73. https://doi.org/10.1158/1078-0432.CCR-05-0165
14. Odri GA, Tchicaya-Bouanga J, Yoon DJY, Modrowski D (2022) Metastatic progression of osteosarcomas: a review of current knowledge of environmental versus oncogenic drivers. Cancers 14:360. https://doi.org/10.3390/cancers14020360
15. Mao X, Mei R, Yu S, Shou L, Zhang W, Li K, Qiu Z, Xie T, Sui X (2022) Emerging technologies for the detection of cancer micrometastasis. Technol Cancer Res Treat 21:1–11. https://doi.org/10.1177/15330338221100355
16. Valenzuela Alvarez M, Gutierrez LM, Correa A, Lazarowski A, Bolontrade MF (2019) Metastatic niches and the modulatory contribution of mesenchymal stem cells and its exosomes. Int J Mol Sci 20(8):1946. https://doi.org/10.3390/ijms20081946
17. Frisbie L, Buckanovich RJ, Coffman L (2022) Carcinoma-associated mesenchymal stem/stromal cells: architects of the pro-tumorigenic tumor microenvironment. Stem Cells 40(8):705–715. https://doi.org/10.1093/stmcls/sxac036
18. Valenzuela Alvarez M, Gutiérrez LM, Auzmendi J, Correa A, Lazarowski A, Bolontrade MF (2020) Acquisition of stem associated-features on metastatic osteosarcoma cells and their functional effects on mesenchymal stem cells. Biochim Biophys Acta Gen Subj. https://doi.org/10.1016/j.bbagen.2020.129522
19. Gutiérrez LM, Valenzuela Alvarez M, Yang Y, Spinelli F, Cantero MJ, Alaniz L, García MG, Kleinerman ES, Correa A, Bolontrade MF (2021) Up-regulation of pro-angiogenic molecules and events do not relate with an angiogenic switch in metastatic osteosarcoma cells but to cell survival features. Apoptosis 26(7–8):447–459. https://doi.org/10.1007/s10495-021-01677-x.20

20. Xu M, Zhang T, Xia R, Wei Y, Wei X (2022) Targeting the tumor stroma for cancer therapy. Mol Cancer 21:208. https://doi.org/10.1186/s12943-022-01670-1
21. Dzobo K, Dandara C (2020) Architecture of cancer-associated fibroblasts in tumor microenvironment: mapping their origins, heterogeneity, and role in cancer therapy resistance. OMICS 24(6):314–339. https://doi.org/10.1089/omi.2020.0023
22. Bolontrade MF, Sganga L, Piaggio E, Viale DL, Sorrentino MA, Robinson A, Sevlever G, García MG, Mazzolini G, Podhajcer OL (2012) A specific subpopulation of mesenchymal stromal cell carriers overrides melanoma resistance to an oncolytic adenovirus. Stem Cells Dev 21:2689–702. https://doi.org/10.1089/scd.2011.0643
23. Sterle HA, Hildebrandt X, Valenzuela Álvarez M, Paulazo MA, Gutierrez LM, Klecha AJ, Cayrol F, Díaz Flaqué MC, Rosemblit C, Barreiro Arcos ML et al (2021) Thyroid status regulates the tumor microenvironment delineating breast cancer fate. Endocr Relat Cancer 28(7):403–418. https://doi.org/10.1530/ERC-20-0277
24. Jia S, Worth LL, Kleinerman ES (1999) A nude mouse model of human osteosarcoma lung metastases for evaluating new therapeutic strategies. Clin Exp Metastasis 17:501–506. https://doi.org/10.1023/a:1006623001465
25. Fritsche-Guenther R, Noske A, Ungethüm U, Kuban RJ, Schlag PM, Tunn PU, Karle J, Krenn V, Dietel M, Sers C (2010) De novo expression of EphA2 in osteosarcoma modulates activation of the mitogenic signalling pathway. Histopathology 57(6):836–850. https://doi.org/10.1111/j.1365-2559.2010.03713.x
26. Kuijjer ML, Rydbeck H, Kresse SH, Buddingh EP, Lid AB, Roelofs H, Bürger H, Myklebost O, Hogendoorn PC, Meza-Zepeda LA et al (2012) Identification of osteosarcoma driver genes by integrative analysis of copy number and gene expression data. Genes Chromosomes Cancer 51(7):696–706. https://doi.org/10.1002/gcc.21956
27. Bielack SS, Kempf-Bielack B, Delling G, Ulrich Exner G, Flege S, Helmke K, Kotz R, Salzer-Kuntschik M, Werner M, Winkelmann W et al (2002) Prognostic factors in high-grade osteosarcoma of the extremities or trunk: an analysis of 1,702 patients treated on neoadjuvant cooperative osteosarcoma study group protocols. J Clin Oncol 20(3):776–790. https://doi.org/10.1200/JCO.2002.20.3.776. Corrected and republished in: J Clin Oncol 2023 Sep 20;41(27):4323–4337
28. Smeland S, Bielack SS, Whelan J, Bernstein M, Hogendoorn P, Krailo MD, Gorlick R, Janeway KA, Ingleby FC, Anninga J et al (2019) Survival and prognosis with osteosarcoma: outcomes in more than 2000 patients in the EURAMOS-1 (European and American Osteosarcoma Study) cohort. Eur J Cancer 109:36–50. https://doi.org/10.1016/j.ejca.2018.11.027
29. Reeves MQ, Balmain A (2023) Mutations, bottlenecks, and clonal sweeps: how environmental carcinogens and genomic changes shape clonal evolution during tumor progression. Cold Spring Harb Perspect Med. https://doi.org/10.1101/cshperspect.a041388
30. Caligiuri G, Tuveson DA (2023) Activated fibroblasts in cancer: perspectives and challenges. Cancer Cell 41(3):434–449. https://doi.org/10.1016/j.ccell.2023.02.015
31. Sharma P, Alsharif S, Fallatah A, Chung BM (2019) Intermediate filaments as effectors of cancer development and metastasis: a focus on keratins, vimentin, and nestin. Cells 8(5):497. https://doi.org/10.3390/cells8050497
32. Sznurkowska MK, Aceto N (2022) The gate to metastasis: key players in cancer cell intravasation. FEBS J 289(15):4336–4354. https://doi.org/10.1111/febs.16046
33. Ali N, Venkateswaran G, Garcia E, Landry T, McColl H, Sergi C, Persad A, Abuetabh Y, Eisenstat DD, Persad S (2019) Osteosarcoma progression is associated with increased nuclear levels and transcriptional activity of activated β-catenin. Genes Cancer 10(3–4):63–79. https://doi.org/10.18632/genesandcancer.191
34. Zhang C, Zhang M, Song S (2018) Cathepsin D enhances breast cancer invasion and metastasis through promoting hepsin ubiquitin-proteasome degradation. Cancer Lett 438:105–15. https://doi.org/10.1016/j.canlet.2018.09.021
35. Gemoll T, Epping F, Heinrich L, Fritzsche B, Roblick UJ, Szymczak S, Hartwig S, Depping R, Bruch HP, Thorns C et al (2015) Increased cathepsin D protein expression is a biomarker for osteosarcomas, pulmonary metastases and other bone malignancies. Oncotarget 6(18):16517–16526. https://doi.org/10.18632/oncotarget.4140
36. Mourão TC, Bezerra SM, de Almeida E, Paula F, Rocha MM, Santos VE, Brazão Junior ES, Abreu D, da Costa WH, Zequi SC (2023) Prognostic role of the immunohistochemical expression of proteins related to the renin-angiotensin system pathway in nonmetastatic clear cell renal cell carcinoma. Urol Oncol 41(8):359.e1-359.e13
37. Seo SU, Woo SM, Im SS, Jang Y, Han E, Kim SH, Lee H, Lee HS, Nam JO, Gabrielson E et al (2022) Cathepsin D as a potential therapeutic target to enhance anticancer drug-induced apoptosis via RNF183-mediated destabilization of Bcl-xL in cancer cells. Cell Death Dis 13(2):115. https://doi.org/10.1038/s41419-022-04581-7
38. Yip HYK, Papa A (2021) Signaling pathways in cancer: therapeutic targets, combinatorial treatments, and new developments. Cells 10(3):659. https://doi.org/10.3390/cells10030659
39. Langley RR, Fidler IJ (2011) The seed and soil hypothesis revisited-the role of tumor–stroma interactions in metastasis to different organs. Int J Cancer 128(11):2527–35. https://doi.org/10.1002/ijc.26031
40. Gao Y, Bado I, Wang H, Zhang W, Rosen JM, Zhang XH (2019) Metastasis organotropism: redefining the congenial soil. Dev Cell 49(3):375–391. https://doi.org/10.1016/j.devcel.2019.04.012
41. Risson E, Nobre AR, Maguer-Satta V, Aguirre-Ghiso JA (2020) The current paradigm and challenges ahead for the dormancy of disseminated tumour cells. Nat Cancer 1(7):672–680. https://doi.org/10.1038/s43018-020-0088-5
42. Fidler IJ (2016) Commentary on "Tumor heterogeneity and the biology of cancer invasion and metastasis." Cancer Res 76(12):3441–2. https://doi.org/10.1158/0008-5472.CAN-16-1330
43. Bolamperti S, Villa I, Rubinacci A (2022) Bone remodeling: an operational process ensuring survival and bone mechanical competence. Bone Res 10:48. https://doi.org/10.1038/s41413-022-00219-8
44. Zhou T, Yang Y, Chen Q, Xie L (2019) Glutamine metabolism is essential for stemness of bone marrow mesenchymal stem cells and bone homeostasis. Stem Cells Int 2019:8928934. https://doi.org/10.1155/2019/8928934
45. Yamada T, Fukasawa K, Horie T, Kadota T, Lyu J, Tokumura K, Ochiai S, Iwahashi S, Suzuki A, Park G et al (2022) The role of CDK8 in mesenchymal stem cells in controlling osteoclastogenesis and bone homeostasis. Stem Cell Rep 17(7):1576–1588. https://doi.org/10.1016/j.stemcr.2022.06.001
46. Bussard KM, Spaeth E, Mutkus LA, Stumpf KA, Marini FC (2017) Mesenchymal stem cell transition to tumor-associated stromal cells contributes to cancer progression. In: Bolontrade MF, Garcia MG (eds) Mesenchymal stromal cells as tumor stromal modulators. Elsevier, Amsterdam, pp 253–73